Journal of
Nanotheranostics

MDPI

Article

Cellular Investigations on Mechanistic Biocompatibility of Green Synthesized Calcium Oxide Nanoparticles with *Danio rerio*

Rashke Eram [1,2], Puja Kumari [2], Pritam Kumar Panda [3], Sonal Singh [2], Biplab Sarkar [4], M. Anwar Mallick [1,2,*] and Suresh K. Verma [3,5,*]

1 University Department of Biotechnology, Vinoba Bhave University, Hazaribagh 825001, India; rashke.eram@gmail.com
2 Advance Science and Technology Research Centre, Vinoba Bhave University, Hazaribagh 825001, India; poojamishra0280@gmail.com (P.K.); sonalsingh1195@gmail.com (S.S.)
3 Department of Physics and Astronomy (Materials Theory), Uppsala University, 75121 Uppsala, Sweden; pritam.panda@physics.uu.se
4 ICAR-Indian Institute of Agricultural Biotechnology (IIAB), IINRG Campus, Namkum Ranchi, Jharkhand 834010, India; biplab_puru@yahoo.co.in
5 School of Biotechnology, KIIT University, Bhubaneswar 751024, India
* Correspondence: amallick1@rediffmail.com (M.A.M.); sureshverma22@gmail.com (S.K.V.)

Abstract: The utility of calcium oxide nanoparticles in the biomedical and physical fields has instigated their biocompatible synthesis and production. Moreover, it is important to investigate their biocompatibility at the molecular level for biomedical and ecotoxicological concern. This study explores the green synthesis of calcium oxide nanoparticles (CaONP) using *Crescentia cujete* leaf extract. The synthesized CaONP were found to have a size of 62 ± 06 nm and a hydrodynamic diameter of 246 ± 12 nm, as determined by FE-SEM and dynamic light scattering (DLS). CaONP was stable in fish medium with a zeta potential of −23 ± 11 mV. The biocompatibility of the CaONP was investigated with adult zebrafish bearing an LC50 of 86.32 µg/mL. Cellular and molecular investigation revealed the mechanism of biocompatibility as a consequence of elicited reactive oxygen species leading to apoptosis, due to accumulation and internalization of CaONP in exposed zebrafish. The study provided detailed information about the mechanistic biocompatibility and a defined horizon of green synthesis of CaONP for biomedical and ecological purposes.

Keywords: calcium oxide nanoparticles; *Danio rerio*; reactive oxygen Species; apoptosis

Citation: Eram, R.; Kumari, P.; Panda, P.K.; Singh, S.; Sarkar, B.; Mallick, M.A.; Verma, S.K. Cellular Investigations on Mechanistic Biocompatibility of Green Synthesized Calcium Oxide Nanoparticles with *Danio rerio*. *J. Nanotheranostics* **2021**, *2*, 51–62. https://doi.org/10.3390/jnt2010004

Received: 3 February 2021
Accepted: 4 March 2021
Published: 9 March 2021

1. Introduction

In recent decades, nanomaterials have been widely applied in different fields of science, such as biotechnology, microbiology, environmental remediation, medicine, various engineering, and material sciences, because of their peculiar properties (e.g., large area to volume ratio) [1,2]. The Food and Drug Administration, United States, has authorized numerous nanomedicines. Many of them have advanced to the concluding stages of development [3]. Calcium oxide nanoparticles are some of the most favored nanomaterials due to their reduced toxicity and excellent physicochemical properties [4]. They are cost-effective, non-corrosive, have good basicity, are environmentally friendly, and manageable [5,6]. Calcium oxide nanoparticles are produced in large amounts in a short time and can be recycled as well [7]. Due to their unique optical and structural properties, they are expedient in applications, such as drug delivery within the body, photothermal therapy, synaptic delivery of chemotherapeutic agents, and photodynamic therapy [8,9]. In addition, controlled size, infiltration into cell and tissue, hindered aggregation by coating, precise contact, and easy dispersion give calcium oxide nanoparticles an advantage over

other metal nanoparticles. They are also involved in storage systems due to their excellent porosity, biocompatibility, and bioactive nature help in gene transfection and drug delivery [10].

Calcium oxide nanoparticles are used as reliable nanoparticles for biomedical purposes [11]. They are effective against microorganisms, such as *Streptococcus aureus, Bacillus cereus, Escherichia coli,* and *Pseudomonas aeruginosa* [7]. Moreover, the antifungal activity of calcium oxide nanoparticles against several fungal strains, such as *Colletotrichum brevisporum* and *Colletotrichum gloeosporioides,* has also been reported [12]. The synthesis and production of calcium oxide nanoparticles have also been increased because of the increasing application. For metal nanoparticles, different synthesis approaches are present, including physical, chemical, and biological methods. Among these, chemical reduction is most preferred, because it is easy, efficient, and cost-effective. Moreover, size and dispersion can be controlled by reforming the experimental factors. However, the use of toxic chemicals poses a great threat of toxicity to every organism. Biological synthesis solves this problem [13]. The biological synthesis of nanoparticles is receiving more acceptance because it is eco-friendly, less toxic, has easily available materials, and pharmacological importance [14]. Green synthesis of calcium oxide nanoparticles using biocompatible green reagents, plants, and microbes (such as bacteria, algae, and fungi) has been reported [6]. Various methods using plants as well as microorganisms have already been described for calcium oxide nanoparticle synthesis [15]. In the present study, *Crescentia cujete L.* leaf extract was used for synthesizing calcium oxide nanoparticles. *Crescentia cujete* is commonly known as the calabash tree, it is a species of a flowering plant that is grown in Africa, Central America, South America, the West Indies, and in the extreme south of Florida [16]. It belongs to the Bignoniaceae family and has a wide range of applications in the medicinal field [17]. According to folk medicine, the pulp of this fruit is used as a laxative and for the treatment of some respiratory problems, such as asthma and catarrh. The bark is utilized in mucoid diarrhea and to clean wounds. The leaves are used as a diuretic, poultice for headaches, hypertension, and to treat tumors and hematomas [18]. The decoction of its fruit is used to treat bronchitis, asthma, cold, cough, stomachaches, diarrhea, urethritis [19]. The leaves of the plant contain naphthoquinones, aucubin, iridoid glycosides, asperuloside, and plumerialumieride [18], with tartaric acid, crescentic acid, cianhidric, tannins, citric acid, alpha and beta marina, beta-sitosterol, triacontanol, apigenin, stigmasterol, *p*-hydroxybenzoyloxy-gluco-esteric acid, 3-hydroxyoctanol glycosides, palmitic acid, and flavonoids-quercetin [20]. The biomolecules and phytochemicals of *Crescentia cujete* are shown to have therapeutic results in different clinical trials [20]. It can be hypothesized that the nanoparticles synthesized using *Crescentia cujete* might possess the properties of *Crescentia cujete* and, therefore, can be used for different medicinal purposes, as well as with high biocompatibility. In addition, the process is an easy, safe, and eco-friendly synthesis method. This study unravels, for the first time, a novel method of synthesizing calcium oxide nanoparticles using the *Crescentia cujete* biomolecules and characterizing their physicochemical properties for biomedical purposes.

It is important to evaluate the biocompatibility of a nanoparticle for utilization in biomedical and environmental applications. The biocompatibility of calcium oxide nanoparticles depends on several factors, such as size, surface modification, shape, biodistribution, structure, concentration, solubility, dosage, biological interactions developed by reactive surfaces bio-availability, histocompatibility, pharmacokinetics, and immunogenicity [21]. Previous literature has reported the toxicity of CaO nanoparticles with different in vitro and in vivo different models; however, a detailed elucidation of the mechanism is lacking [21]. Given these facts, the current study also evaluates the biocompatibility of synthesized nanoparticles using the zebrafish model, which is an established animal modal for biocompatibility because of its short developing time, transparency, and high genetic similarities with humans. The biocompatibility assessment has been done by determination of the effect of the synthesized nanoparticles on development and cellular changes.

2. Materials and Methods

2.1. Green Synthesis of Calcium Oxide Nanoparticles

Calcium oxide nanoparticle green synthesis was carried out by using *Crescentia cujete* leaf extract as the reducing agent and calcium chloride as the metal salt precursor. For the preparation of aqueous leaf extract of *Crescentia cujete*, fresh leaves of *Crescentia cujete* were collected from the Botanical garden, Vinoba Bhave University, Hazaribagh, India, and washed thoroughly with tap water, followed by distilled water, to remove any grime material. These were cut into small pieces and air-dried at room temperature. The extract was prepared by adding 10 g of the leaf to 100 mL distilled water and boiled for 20 min. The extract was then filtered twice using Whatman No. 1 filter paper to get clear extract. The reaction solution was prepared by mixing an aqueous solution of 1 mM calcium chloride ($CaCl_2$) to the leaf extract in a 1:1 ratio and left undisturbed for 24 h at room temperature. After 24 h, the solution was washed thrice by centrifugation at 5000 rpm for 15 min and the pellet containing the CaONP was dried in a hot air oven to obtain the CaONP powder.

2.2. Physiochemical Characterization

The physiochemical characterizations of CaONP were done using standard techniques. UV-Vis spectroscopy was done to determine the optical properties of the nanoparticles. The scanning was performed through UV-visible spectrophotometer (Cary 5000, Agilent, Santa Clara, CA, USA) by scrutinizing the spectral scan at a range of 200–800 nm. Further, the hydrodynamic size and zeta potential of the CaONP was determined in the fish medium through dynamic light scattering (DLS) using Zetasizer (Malvern, UK). The size of the CaONP was further determined by electron microscopy by using FE-SEM (Carl Zeiss, Jena, Germany). The samples were dried in the hot sun and were imaged at 20 KV.

2.3. Zebrafish Maintenance

The adult zebrafish were maintained in an aquarium system purchased from the local market of Hazaribagh, Jharkhand, India. For maintenance of the physiological parameters, fish water containing 75 g $NaHCO_3$, 18 g sea salt, 8.4 g $CaSO_4$ per 1000 mL was regulated in the system [22]. Fish feeding was done thrice a day, with bloodworm containing fish food. The associated guidelines of VBU University's Institutional Animal Ethics Committee (IAEC) were applied for all animal procedures. All animal procedures were approved by the relevant guidelines of the VBU University's Institutional Animal Ethics Committee (IAEC). All studies were performed in compliance with applicable animal management standards and IAEC, VBU University regulations.

2.4. Toxicological Study

Toxicological estimation of CaONP was observed in adult zebrafish. The nanoparticle was characterized for size and charge. For the toxicological study, 3-month-old fish of proportionate sizes were exposed to varying concentrations of CaONP (10, 25, 50, 100, 200 µg/mL) in 200 mL of filter-sterilized fish water [23]. The experiment was carried out for 96 h. The morphological abnormalities were observed, photographs were taken, and the mortality rate was calculated. All of the experiments were conducted in triplicates, and data were presented as mean ± SD. The statistical analysis was done through one-way ANOVA analysis.

2.5. Uptake Analysis and Oxidative Stress Assessment

CaONP uptake in adult zebrafish was evaluated by measuring the change in granularity through side scatter measurement by flow cytometry [24]. The reactive oxygen species (ROS) intensity in zebrafish exposed to different CaONP was measured for oxidative stress analysis. After 96 h of exposure, the fish were sacrificed, their muscles and intestines were dissected, and the cell suspension was made by sonication. The debris was removed by centrifugation at 5000 rpm for 10 min. Then, the cell suspension was stained by 1.25 µg/mL H_2DCFDA dye for 20 min in dark. The extra stain was removed by

centrifugation. The side scatter analysis and the fluorescent intensity measurement were estimated using Attune Next Gen flow cytometer (Thermo Scientific, Grand Island, NY, USA). The fluorescent intensity of DCFDA was measured using the BL1 filter of the system. All of the experiments were performed in triplicates and statistical analysis was performed using Graph pad prism 8. The data were presented as mean ± SD. The statistical analysis was done through one-way ANOVA analysis.

2.6. Apoptosis Analysis

For Apoptotic analysis of adult zebrafish exposed to CaONP, acridine orange dye was used, and the method described by Verma et al was followed [25]. For cell suspension preparation, muscles and intestine were dissected after 96 h of exposure and sonicated. The debris was removed by centrifugation at 5000 rpm for 10 min. The cell suspension was stained with 5 µg/mL acridine orange (AO), dissolved in HF for 20 min in the dark. The extra stain was removed by centrifugation. The stained cell suspension was imaged using the green channel of EVOS inverted fluorescent microscope (Thermo Scientific, USA).

3. Results and Discussion

3.1. Green Synthesis and Characterization of CaONP

The green synthesis of calcium oxide nanoparticles (CaONP) was carried out by using *Crescentia cujete* leaf extract as shown in Figure 1. The synthesized nanoparticles were dried and suspended in an HF medium for characterization. The HF medium was selected for suspension preparation following the medium used for the biological assays. The nanoparticles were characterized for their physical and optical properties as shown in Figure 2A. The UV-Vis spectrum analysis exhibited a sharp peak. The exhibition of absorbance peak was reported as being distinguished properties of nanoparticles to classify their optical properties [26]. Green synthesized CaONP showed peak absorbance at 287 nm. Previous reports have also described the possession of peak at a range of 280–300 nm, in the case of CaO nanoparticles synthesized by other procedures [6]. The stability of the nanoparticles in the HF medium was further checked using dynamic light scattering by determining their zeta potential. As shown in Figure 2B, the CaONP was found to have a zeta potential of -23 ± 11 mV in HF medium, which indicated the stability of CaONP. The size of the nanoparticles was further determined through different techniques. As shown in Figure 2C, FE-SEM analysis of synthesized CaONP showed a size of 62 ± 6 nm. The hydrodynamic diameter of the nanoparticles was found to be 246 ± 12 nm (Figure 2D). The difference in the size of the nanoparticles determined by DLS and FE-SEM can be attributed to the attached water and salt molecules to the nanoparticles present in the HF buffer medium [27]. The physicochemical characterization of the nanoparticles confirmed their nano properties and successful synthesis of nanoparticles. With reference to the previous literatures and obtained experimental results, it can be confirmed that the CaO nanoparticles synthesized from the leaf extract of *Crescentia cujete* was stable in the HF medium with a size of a nanometer. These physiochemical properties of CaONP can be argued to affect the biological properties of nanoparticles.

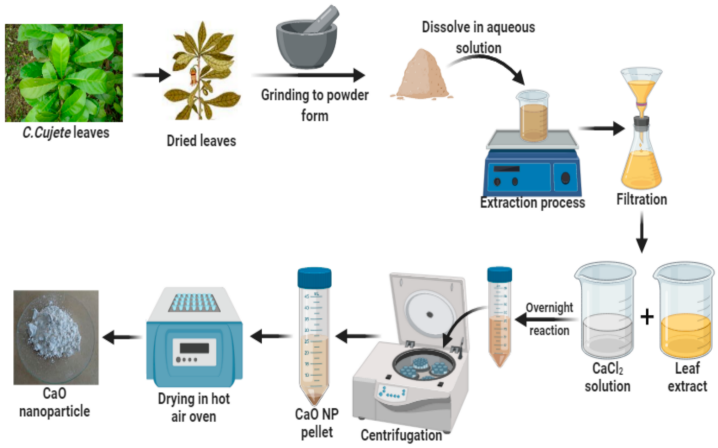

Figure 1. Schematic presentation of green synthesis CaONP using *C. Cujete* leaf extract. The extract was prepared from the freshly collected leaves. The synthesized CaONP was further characterized for its physicochemical properties.

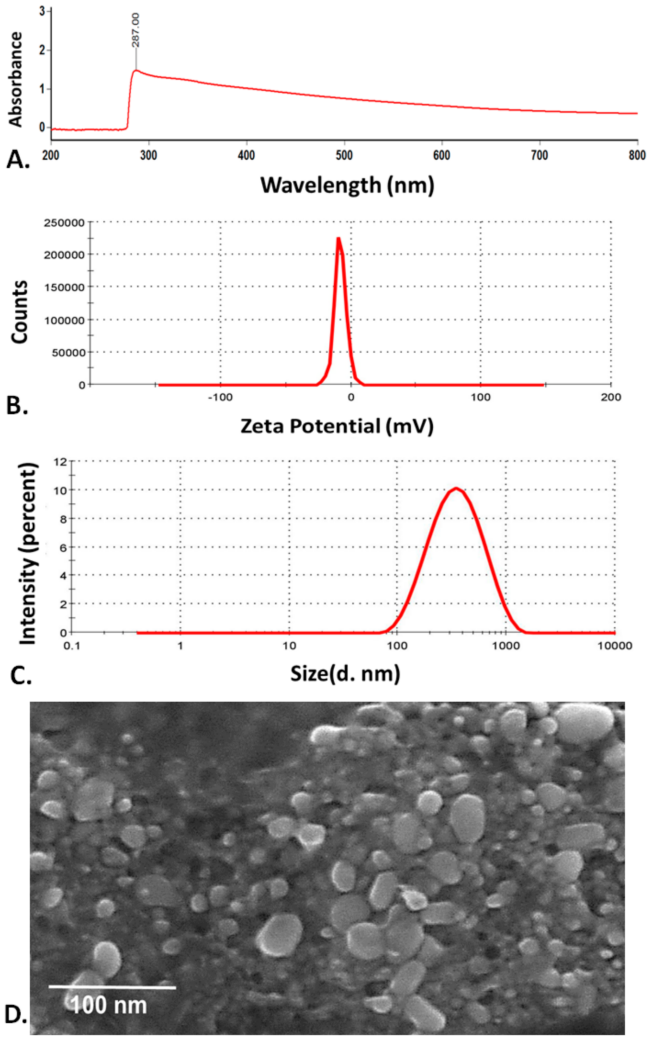

Figure 2. Physiochemical characterization of green synthesized CaONP. (**A**) UV–Vis spectrum of CaONP; (**B**) zeta-potential of CaONP determined by dynamic light scattering; (**C**) hydrodynamic diameter of CaONP as determined by dynamic light scattering; (**D**) optical image of CaONP as determined by FE-SEM.

3.2. In Vivo Biocompatibility of Green Synthesized CaONP

The biocompatibility and eco-compatibility of a nanoparticle is an important factor to determine their potential utility for different biomedical or ecological applications [28]. The nanoparticles are assumed to be delivered and exposed to the living system through the topical path—either in the ecological system, such as natural water bodies, or during their exposure to the body for biomedical purposes. The living system is assumed to be exposed through the topical pathway, i.e., through skin surface, which can further direct to the internal tissues and cells. Hence, it is important to determine the in vivo effect of nanoparticles exhibited due to their accumulation at the cell surface as well as internalization inside the cells. To determine the biocompatibility of synthesized CaONP, an in vivo study was performed with zebrafish. The nanoparticles were checked for their effect on the metabolism and survivability of adult zebrafish. As shown in Figure 3A, the percentage survivability of zebrafish was found to be concentration and time-dependent exposure of CaO nanoparticles. Interestingly, the mortality was increasing at a higher rate in the case of 50 μg/mL and above. Figure 3B–D showed the survivability percentage of zebrafish exposed to different concentrations of CaONP at 24 h, 48 h, and 96 h exposure. As observed, the CaONP showed their highest lethal effect after the exposure of 72 h. The LC50 was calculated as 86.32 μg/mL for 72 h. The mortality effect can be attributed to the accumulation of nanoparticles on the surface of the outer shell of zebrafish, which further can be accounted for their absorption inside cells, creating the lethal effect [23]. The accumulation of the nanoparticles on the surface can be correlated with their physiochemical properties, such as the zeta potential and surface coating [29]. The biologically synthesized CaONP was tested for a zeta potential of -23 ± 11 mV. The negative charge can be attributed to their attachment with the skin surface, and gradient produced due to accumulation can be accounted for their internalization inside the cells. Moreover, it can be argued that the nanoparticles surface had acquired these charges due to the presence of coated biomolecules on the surface of nanoparticles and the protein corona [30]. It can also be argued that the nanoparticles would have been taken inside the body through the oral path, creating a lethal effect on the intestinal tissue, as well as on other internal organs through assimilation [31]. With reference to these facts, it can be inferred that the properties of green synthesized CaONP were playing an important role in the biocompatibility of nanoparticles.

The assumption was further checked by the visual analysis of fishes exposed to different concentrations of CaONP. As shown in Figure 4, the accumulation of nanoparticles on the surface was visible in the form of black spots. The formation of lesions was observed in fishes exposed to higher concentrations of CaONP and the overall health of the fishes was found to have deteriorated. Interestingly, the detrimental effects were higher with the increase in exposure time. Similar effects have been reported to be observed in adult zebrafishes exposed to other metallic oxide nanoparticles, such as MgONP, in our previous studies [14]. With the visual observation and the experimental analysis, it was determined that the nanoparticles were showing the toxic effect in a dose-dependent manner. The results indicated to the effective role of concentration of CaONP. It can be argued that the physiochemical properties, such as charge, size, and nanoparticle coating were altogether influenced by the increase in concentration of the nanoparticles leading to the cytotoxic effects [32,33]. However, the analysis raised eagerness to the mechanism. Previous literature has reported the bio-toxic effects of nanoparticles in zebrafish due to the metabolic changes at the molecular level. The nanoparticles have been reported to interact with the different proteins at the cellular level influential in the metabolic process in cells [21]. It has been told that the nanoparticles internalize inside the cells and interact with oxidative stress proteins, such as Sod1 and P53, to influence the phenomenon of oxidative stress and cell death [34]. Concerning these facts, the effect of synthesized CaONP to the zebrafish was checked through experimental analysis.

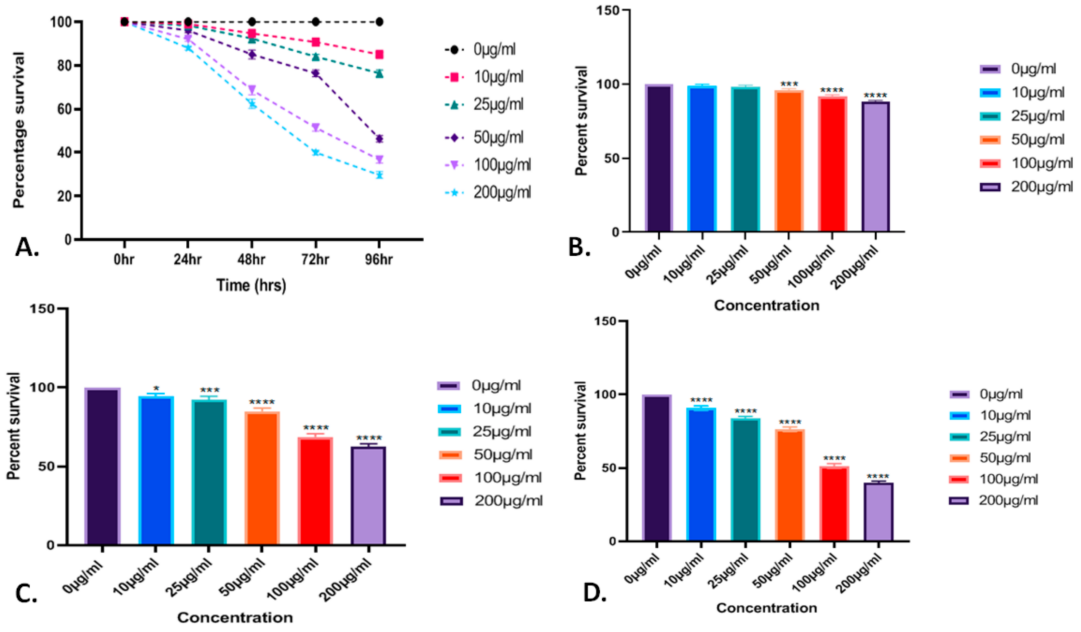

Figure 3. Cytotoxicity analysis of CaONP with adult Zebrafish. (**A**) Survivability of zebrafish exposed to CaONP at different time points. Percentage survivability of zebrafish exposed to different concentrations of CaONP at (**B**) 24 h, (**C**) 48 h, (**D**) 96 h. A group of five adult zebrafish was taken for adult fish studies. The values represent the mean ± SD of three independent experiments. The *p*-values were obtained for post hoc analysis (Tukey). **** $p < 0.001$, *** $p < 0.05$, ** $p < 0.05$, * $p < 0.05$ denotes compared significant change at each exposed concentration as obtained from post hoc analysis after one-way ANOVA.

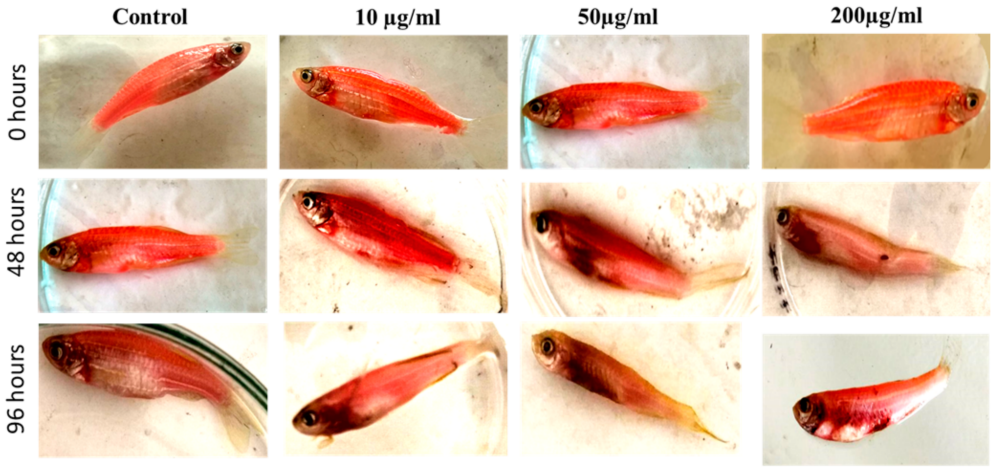

Figure 4. Morphological change observation of adult zebrafish exposed to CaONP with adult Zebrafish. The fish were exposed to different concentrations of CaONP at a time point of 24 h, 48 h, and 96 h. The formation of the lesion with an accumulation of nanoparticles was observed.

The zebrafish cells treated with CaONP were first analyzed for the accumulation and internalization of nanoparticles. As shown in Figure 5A,B, the mean side scatter analysis of the cells treated with CaONP showed a significant dose-dependent increase in intensity. Variation in side scatter in cells determined by flow cytometry has been reported to be a proven technique to determine the qualitative internalization of nanoparticles inside the cells [35]. An increase in mean side scatter of cells exposed with increasing concentration of CaONP interpreted to the dose-dependent internalization of nanoparticles. Further, it was estimated that the internalized nanoparticles were leading to the imbalance in oxidative stress in cells through induction of uncontrolled intensity of reactive oxygen species (ROS) [14]. The fact was crisscrossed by the flow cytometry investigation of

zebrafish cells stained with DCFDA. DCFDA has been recognized as the indicator of peroxide ion produced inside the cells [36] due to their nature of binding with peroxide ions (ROS) and fluorescence of green color [37]. As shown in Figure 5C,D, the fluorescence of DCFDA was found to be increased with an increase in exposure concentration of CaONP to zebrafish cells. The data interpreted towards the dose-dependent production of ROS by nanoparticle exposure in zebrafish. The inferred result can be attributed to the fact that the internalized nanoparticles inside the cells of zebrafish would have to interact with oxidative stress metabolism proteins, such as Sod1, Sod2, leading to their abnormal activity [14]. The structural and functional influence of the nanoparticles due to the interaction were leading to the imbalance in the function of cell organelles like mitochondria. The imbalance caused the abnormal production of ROS inside the cells.

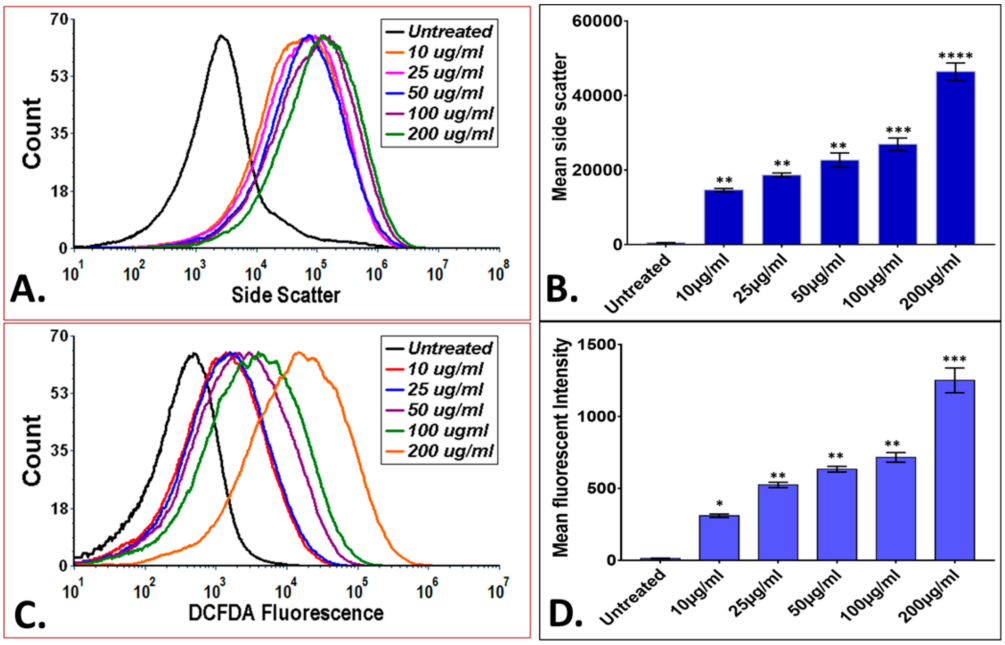

Figure 5. Flow cytometry analysis of cellular changes in adult zebrafish exposed to CaONP. (**A**) Side scatter analysis indicated the internalization of nanoparticles; (**B**) bar graph presentation of mean side scatter in cells exposed to CaONP for 96 h. (**C**) DCFDA fluorescence intensity presenting the induction of reactive oxygen species (ROS) in zebrafish cells exposed to different concentrations of CaONP at 96 h. (**D**) Bar graph presentation of mean fluorescent intensity of DCFDA to determine the significant difference in ROS production in cells exposed to CaONP for 96 h. The values represent the mean ± SEM of three independent experiments. Ns; non-significance, * $p < 0.001$, ** $p < 0.001$, *** $p < 0.001$, denotes compared significant change at each exposed concentration as obtained from post hoc analysis after one-way ANOVA.

Further, it has been reported that the imbalance in ROS inside the cells and dysregulation inactivity of program cell death proteins plays an important role in the apoptosis of cells [38]. It was estimated that the zebrafish cells exposed to CaONP would have been affected by the abnormal production of ROS and causing the abnormal increase in apoptosis of cells. The fact was experimentally checked by the fluorescent microscopy through analysis of acridine orange fluorescence in zebrafish exposed to different concentrations of CaONP. Acridine orange has been reported to bind with the grooves of DNA in cells with the fluorescence of green color [39]. Hence, the apoptosis in cells can be interpreted from the green fluorescence of acridine orange stained cells exposed to nanoparticles. As shown in Figure 6, the green fluorescence intensity of acridine orange was found to increase with an increase in the exposed concentration of CaONP. The observed result can be attributed to the higher apoptosis in zebrafish with exposure to the higher concentration of CaONP. The apoptosis dysregulation can also be argued to the interaction of internalized nanoparticles with apoptosis regulation proteins, such as caspases and P53 [21].

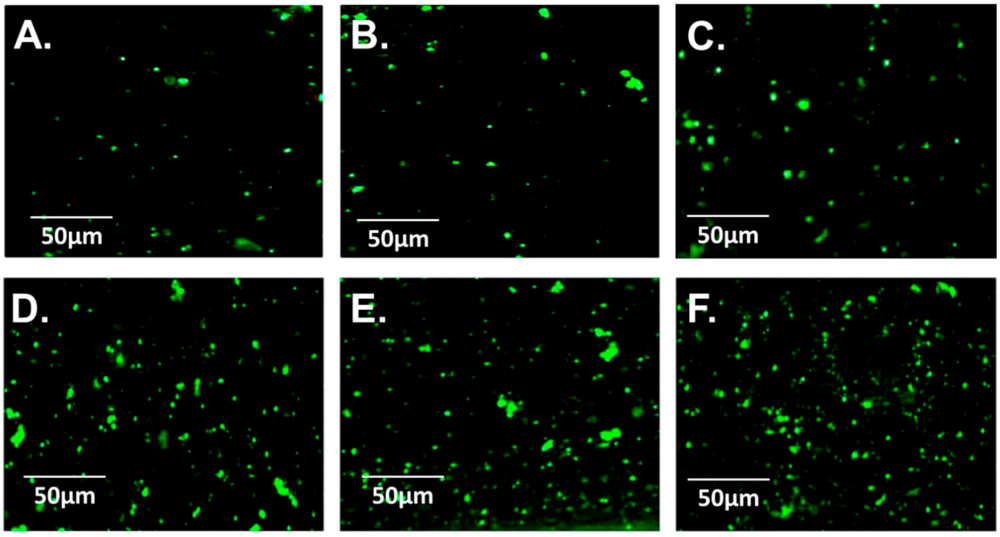

Figure 6. Fluorescent microscopy analysis of apoptosis in adult zebrafish exposed to CaONP. The image presents the green fluorescent intensity of acridine orange in zebrafish cells exposed to different concentrations of CaONP. (**A**) Untreated, (**B**) 10 µg/mL, (**C**) 25 µg/mL, (**D**) 50 µg/mL, (**E**) 100 µg/mL, (**F**) 200 µg/mL. The suspension of cells was obtained by sonicating the zebrafish muscle cells exposed to different concentrations of nanoparticles.

Hence, concerning previous literature and our experimental results, the mechanism of the biocompatibility of CaONP with zebrafish can be deduced as an effect of accumulation and internalization of CaONP inside the body of zebrafish. The internalized nanoparticles were interacting with the oxidative stress metabolism and apoptosis proteins, such as Sod1 and P53. The interaction leads to higher production of ROS inside the cells guiding their apoptosis. Moreover, the combined effect of CaONP–P53 interactions and ROS were also leading to the apoptosis of cells.

The study deduced the mechanism of biocompatibility of CaONP with adult zebrafish at the cellular level. The information deduced from the results will provide direction to explore the mechanism of CaONP at molecular level. The future research can be directed to modify the properties of nanoparticles using the biomolecules explored for the mechanism of toxicity for higher biocompatibility. The study also explored the novel method of the green production of CaONP using medicinal plant extract for biomedical purposes and excavated the future path of research to explore the potential use of biomolecules extracted from *Crescentia cujete* for synthesis of other biocompatible metal nanoparticles.

4. Conclusions

As shown in Figure 7, successful green synthesis and characterization of CaONP was performed. The synthesized CaONP was found to be stable with a size of 52 nm. The 52 nm CaONP was well characterized for their optical properties by showing SPR at 287 nm. The synthesized CaONP were found to be biocompatible at a specific range of concentrations with Zebrafish. Moreover, the molecular mechanism of CaONP biocompatibility was deduced as a result of apoptosis in cells due to induced ROS by the exposure. The study guided to the green production of CaONP for higher biocompatibility. Moreover, a green approach for the production of CaONP was also deduced by the use of the medicinal plant.

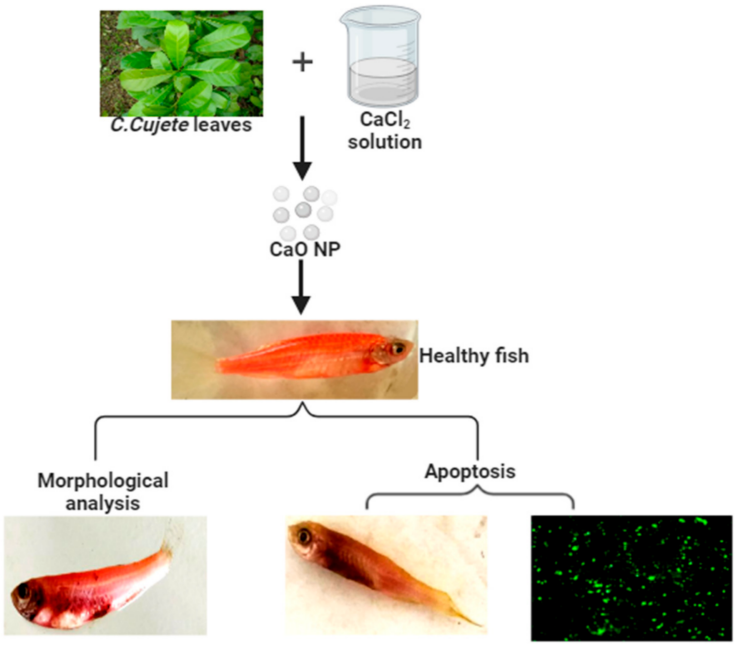

Figure 7. Schematic presentation of the study.

Author Contributions: Conceptualization, S.K.V.; Data curation, M.A.M. and S.K.V.; Formal analysis, P.K., M.A.M. and S.K.V.; Funding acquisition, S.K.V.; Investigation, R.E., P.K., S.S. and S.K.V.; Methodology, R.E., P.K. and S.K.V.; Project administration, S.K.V.; Resources, S.K.V.; Software, P.K.P. and S.K.V.; Supervision, M.A.M. and S.K.V.; Validation, R.E., S.S., B.S., M.A.M. and S.K.V.; Visualization, S.S. and S.K.V.; Writing—original draft, R.E., S.S., B.S. and S.K.V.; Writing—review & editing, P.K.P. and S.K.V. All authors have read and agreed to the published version of the manuscript.

Funding: This research received no external funding.

Institutional Review Board Statement: The study was conducted according to the guidelines of the Declaration of Helsinki, and approved by Institutional Animal Ethics Committee (IAEC) of VBU University. All experiments were performed in accordance with relevant animal practice guidelines and regulations of IAEC, VBU University (VBU/IAEC/2018/MEET-1/A3).

Data Availability Statement: Not applicable.

Acknowledgments: The author acknowledges zebrafish facility of Advance Science and Technology Research Centre and their staff for providing full support during the zebrafish experiments.

Conflicts of Interest: The authors declare no conflict of interest.

References

1. Mueller, N.C.; Nowack, B. Nanoparticles for remediation: Solving big problems with little particles. *Elements* **2010**, *6*, 395–400. [CrossRef]
2. Kumar, R.; Mondal, K.; Panda, P.K.; Kaushik, A.; Abolhassani, R.; Ahuja, R.; Rubahn, H.G.; Mishra, Y.K. Core-shell nanostructures: Perspectives towards drug delivery applications. *J. Mater. Chem. B* **2020**, *8*, 8992–9027. [CrossRef]
3. Prakash, J.; Parveen, A.; Mishra, Y.K.; Kaushik, A. Nanotechnology-assisted liquid crystals-based biosensors: Towards fundamental to advanced applications. *Biosens. Bioelectron.* **2020**, *168*, 112562. [CrossRef] [PubMed]
4. Ferraz, E.; Gamelas, J.A.F.; Coroado, J.; Monteiro, C.; Rocha, F. Eggshell waste to produce building lime: Calcium oxide reactivity, industrial, environmental and economic implications. *Mater. Struct. Constr.* **2018**, *51*, 115. [CrossRef]
5. Bano, S.; Pillai, S. Green synthesis of calcium oxide nanoparticles at different calcination temperatures. *World J. Sci. Technol. Sustain. Dev.* **2020**, *17*, 283–295. [CrossRef]
6. Anantharaman, A.; George, M. Green Synthesis of Calcium Oxide Nanoparticles and Its Applications. *J. Eng. Res. Appl.* **2016**, *6*, 27–31.
7. Abo-zeid, Y.; Williams, G.R. The potential anti-infective applications of metal oxide nanoparticles: A systematic review. *Wiley Interdiscip. Rev. Nanomed. Nanobiotechnol.* **2020**, *12*, e1592. [CrossRef]

8. Canaparo, R.; Foglietta, F.; Limongi, T.; Serpe, L. Biomedical applications of reactive oxygen species generation by metal nanoparticles. *Materials* **2021**, *14*, 53. [CrossRef]
9. Ranghar, S.; Sirohi, P.; Verma, P.; Agarwal, V. Nanoparticle-based drug delivery systems: Promising approaches against infections. *Braz. Arch. Biol. Technol.* **2013**, *57*, 209–222. [CrossRef]
10. Sinha, S.; Aman, A.K.; Kr. Singh, R.; Kr, N.; Shivani, K. Calcium oxide(CaO) nanomaterial (Kukutanda twak Bhasma) from egg shell: Green synthesis, physical properties and antimicrobial behaviour. *Mater. Today Proc.* **2020**. [CrossRef]
11. Som, A.; Raliya, R.; Paranandi, K.; High, R.A.; Reed, N.; Beeman, S.C.; Brandenburg, M.; Sudlow, G.; Prior, J.L.; Akers, W.; et al. Calcium carbonate nanoparticles stimulate tumor metabolic reprogramming and modulate tumor metastasis. *Nanomedicine* **2019**, *14*, 169–182. [CrossRef]
12. Maringgal, B.; Hashim, N.; Tawakkal, I.S.M.A.; Hamzah, M.H.; Mohamed, M.T.M. Biosynthesis of CaO nanoparticles using Trigona sp. Honey: Physicochemical characterization, antifungal activity, and cytotoxicity properties. *J. Mater. Res. Technol.* **2020**, *9*, 11756–11768. [CrossRef]
13. Verma, S.K.; Jha, E.; Panda, P.K.; Thirumurugan, A.; Suar, M. Biological Effects of Green-Synthesized Metal Nanoparticles: A Mechanistic View of Antibacterial Activity and Cytotoxicity. In *Advanced Nanostructured Materials for Environmental Remediation*; Springer: Cham, Switzerland, 2019; pp. 145–171.
14. Verma, S.K.; Nisha, K.; Panda, P.K.; Patel, P.; Kumari, P.; Mallick, M.A.; Sarkar, B.; Das, B. Green synthesized MgO nanoparticles infer biocompatibility by reducing in vivo molecular nanotoxicity in embryonic zebrafish through arginine interaction elicited apoptosis. *Sci. Total Environ.* **2020**, *713*, 136521. [CrossRef]
15. Jagadeesh, D.; Prashantha, K.; Shabadi, R. Star-shaped sucrose-capped CaO nanoparticles from Azadirachta indica: A novel green synthesis. *Inorg. Nano-Metal Chem.* **2017**, *47*, 708–712. [CrossRef]
16. Kaneko, T.; Ohtani, K.; Kasai, R.; Yamasaki, K.; Nguyen Minh, D. n-Alkyl glycosides and p-hydroxybenzoyloxy glucose from fruits of Crescentia cujete. *Phytochemistry* **1998**, *47*, 259–263. [CrossRef]
17. Parvin, M.S.; Das, N.; Jahan, N.; Akhter, M.A.; Nahar, L.; Islam, M.E. Evaluation of in vitro anti-inflammatory and antibacterial potential of Crescentia cujete leaves and stem bark Pharmacology and Toxicology. *BMC Res. Notes* **2015**, *8*, 412. [CrossRef] [PubMed]
18. Das, N.; Islam, M.E.; Jahan, N.; Islam, M.S.; Khan, A.; Islam, M.R.; Parvin, M.S. Antioxidant activities of ethanol extracts and fractions of Crescentia cujete leaves and stem bark and the involvement of phenolic compounds. *BMC Complement. Altern. Med.* **2014**, *14*, 45. [CrossRef] [PubMed]
19. Morton, J.F. The calabash (Crescentia cujete) in folk medicine. *Econ. Bot.* **1968**, *22*, 273–280. [CrossRef]
20. Olaniyi, M.B.; Lawal, I.O.; Olaniyi, A.A. Proximate, phytochemical screening and mineral analysis of *Crescentia cujete* L. leaves. *J. Med. Plants Econ. Dev.* **2018**, *2*, 1–7. [CrossRef]
21. Kumari, S.; Kumari, P.; Panda, P.K.; Patel, P.; Jha, E.; Mallick, M.A.; Suar, M.; Verma, S.K. Biocompatible biogenic silver nanoparticles interact with caspases on an atomic level to elicit apoptosis. *Nanomedicine* **2020**. [CrossRef]
22. Patel, P.; Panda, P.K.; Kumari, P.; Singh, P.K.; Nandi, A.; Mallick, M.A.; Das, B.; Suar, M.; Verma, S.K. Selective in vivo molecular and cellular biocompatibility of black peppercorns by piperine-protein intrinsic atomic interaction with elicited oxidative stress and apoptosis in zebrafish eleuthero embryos. *Ecotoxicol. Environ. Saf.* **2020**, *192*, 110321. [CrossRef]
23. Sheel, R.; Kumari, P.; Panda, P.K.; Jawed Ansari, M.D.; Patel, P.; Singh, S.; Kumari, B.; Sarkar, B.; Mallick, M.A.; Verma, S.K. Molecular intrinsic proximal interaction infer oxidative stress and apoptosis modulated in vivo biocompatibility of P.niruri contrived antibacterial iron oxide nanoparticles with zebrafish. *Environ. Pollut.* **2020**, *267*, 115482. [CrossRef]
24. Verma, S.K.; Jha, E.; Panda, P.K.; Kumari, P.; Pramanik, N.; Kumari, S.; Thirumurugan, A. Molecular investigation to RNA and protein based interaction induced in vivo biocompatibility of phytofabricated AuNP with embryonic zebrafish. *Artif. Cells, Nanomedicine Biotechnol.* **2018**, *46*, S671–S684. [CrossRef]
25. Verma, S.K.; Jha, E.; Panda, P.K.; Mukherjee, M.; Thirumurugan, A.; Makkar, H.; Das, B.; Parashar, S.K.S.; Suar, M. Mechanistic insight into ROS and neutral lipid alteration induced toxicity in the human model with fins (Danio rerio) by industrially synthesized titanium dioxide nanoparticles. *Toxicol. Res.* **2018**, *7*, 244–257. [CrossRef]
26. Verma, S.K.; Jha, E.; Kiran, K.J.; Bhat, S.; Suar, M.; Mohanty, P.S. Synthesis and characterization of novel polymer-hybrid silver nanoparticles and its biomedical study. *Mater. Today Proc.* **2016**, *3*, 1949–1957. [CrossRef]
27. Berg, J.M.; Romoser, A.; Banerjee, N.; Zebda, R.; Sayes, C.M. The relationship between pH and zeta potential of ∼ 30 nm metal oxide nanoparticle suspensions relevant to in vitro toxicological evaluations. *Nanotoxicology* **2009**, *3*, 276–283. [CrossRef]
28. Jha, E.; Panda, P.K.; Patel, P.; Kumari, P.; Mohanty, S.; Parashar, S.; Ahuja, R.; Verma, S.K.; Suar, M. Intrinsic atomic interaction at molecular proximal vicinity infer cellular biocompatibility of antibacterial nanopepper. *Nanomedicine* **2021**. [CrossRef] [PubMed]
29. Schaeublin, N.M.; Braydich-Stolle, L.K.; Schrand, A.M.; Miller, J.M.; Hutchison, J.; Schlager, J.J.; Hussain, S.M. Surface charge of gold nanoparticles mediates mechanism of toxicity. *Nanoscale* **2011**, *3*, 410–420. [CrossRef]
30. Corbo, C.; Molinaro, R.; Parodi, A.; Toledano Furman, N.E.; Salvatore, F.; Tasciotti, E. The impact of nanoparticle protein corona on cytotoxicity, immunotoxicity and target drug delivery. *Nanomedicine* **2016**, *11*, 81–100. [CrossRef] [PubMed]
31. Verma, S.K.; Jha, E.; Kumar Panda, P.; Mishra, A.; Thirumurugan, A.; Das, B.; Parashar, S.; Suar, M. Rapid novel facile biosynthesized Silver nanoparticles from Bacterial release induce biogenicity and concentration dependent in vivo cytotoxicity with embryonic Zebrafish—A mechanistic insight. *Toxicol. Sci.* **2018**, *161*, 125–138. [CrossRef]

32. Sukhanova, A.; Bozrova, S.; Sokolov, P.; Berestovoy, M.; Karaulov, A.; Nabiev, I. Dependence of Nanoparticle Toxicity on Their Physical and Chemical Properties. *Nanoscale Res. Lett.* **2018**, *13*, 44. [CrossRef] [PubMed]
33. Silva, T.; Pokhrel, L.R.; Dubey, B.; Tolaymat, T.M.; Maier, K.J.; Liu, X. Particle size, surface charge and concentration dependent ecotoxicity of three organo-coated silver nanoparticles: Comparison between general linear model-predicted and observed toxicity. *Sci. Total Environ.* **2014**, *468–469*, 968–976. [CrossRef] [PubMed]
34. Kumari, P.; Panda, P.K.; Jha, E.; Pramanik, N.; Nisha, K.; Kumari, K.; Soni, N.; Mallick, M.A.; Verma, S.K. Molecular insight to in vitro biocompatibility of phytofabricated copper oxide nanoparticles with human embryonic kidney cells. *Nanomedicine* **2018**, *13*, 2415–2433. [CrossRef]
35. Verma, S.K.; Jha, E.; Panda, P.K.; Thirumurugan, A.; Parashar, S.K.S.; Patro, S.; Suar, M. Mechanistic Insight into Size-Dependent Enhanced Cytotoxicity of Industrial Antibacterial Titanium Oxide Nanoparticles on Colon Cells Because of Reactive Oxygen Species Quenching and Neutral Lipid Alteration. *ACS Omega* **2018**, *3*, 1244–1262. [CrossRef] [PubMed]
36. Eruslanov, E.; Kusmartsev, S. Identification of ROS using oxidized DCFDA and flow-cytometry. *Methods Mol. Biol.* **2010**, *594*, 57–72.
37. Verma, S.K.; Jha, E.; Panda, P.K.; Das, J.K.; Thirumurugan, A.; Suar, M.; Parashar, S. Molecular aspects of core-shell intrinsic defect induced enhanced antibacterial activity of ZnO nanocrystals. *Nanomedicine* **2017**, *13*, 43–68. [CrossRef]
38. Kumari, P.; Panda, P.K.; Jha, E.; Kumari, K.; Nisha, K.; Mallick, M.A.; Verma, S.K. Mechanistic insight to ROS and Apoptosis regulated cytotoxicity inferred by Green synthesized CuO nanoparticles from Calotropis gigantea to Embryonic Zebrafish. *Sci. Rep.* **2017**, *7*, 16284. [CrossRef]
39. Tucker, B.; Lardelli, M. A rapid apoptosis assay measuring relative acridine orange fluorescence in zebrafish embryos. *Zebrafish* **2007**, *4*, 113–116. [CrossRef] [PubMed]